

Radio frequency interference shielding and mitigation techniques for a sensitive search for the 327 MHz line of deuterium

Alan E. E. Rogers, Preethi Pratap, and Joseph C. Carter

Haystack Observatory, Massachusetts Institute of Technology, Westford, Massachusetts, USA

Marcos A. Diaz

Department of Electrical and Computer Engineering, Boston University, Boston, Massachusetts, USA

Received 19 August 2004; revised 5 January 2005; accepted 10 March 2005; published 25 June 2005.

[1] An array of 24 stations, each with 24 crossed dipoles, has been built at the Haystack Observatory in Westford, Massachusetts. This array has been designed to make a sensitive search for the 327 MHz spectral line of deuterium. Since the deuterium line is expected to be about 50 dB weaker than the 1420 MHz hydrogen line, the amelioration of radio frequency interference (RFI) is a major challenge for the performance of the deuterium array. Locally generated RFI from the array and from nearby sites has been reduced by extensive shielding and in some cases by the removal of consumer electronics, like certain digital answering machines that emit strong signals in the 327.3–327.5 MHz band, which is of prime importance for the search. Since almost all the RFI comes from the horizon, the station array has parasitic directors added to the dipoles to reduce the response at the horizon. An RFI monitor with 12 active Yagi antennas pointed every 30° in azimuth provides a way of determining the direction of the RFI and yields information on frequencies and time spans that need to be excised from the array data. We describe the RFI excision techniques and the levels of spectral and continuum RFI measured at the observatory.

Citation: Rogers, A. E. E., P. Pratap, J. C. Carter, and M. A. Diaz (2005), Radio frequency interference shielding and mitigation techniques for a sensitive search for the 327 MHz line of deuterium, *Radio Sci.*, 40, RS5S17, doi:10.1029/2004RS003157.

1. Introduction

[2] Starting in the late 1950s and early 1960s, the detection of deuterium in interstellar gas has been considered one of the most important efforts in radio astronomy. Its measurement constrains the photon-to-baryon ratio, and hence the cosmological baryon density. This measurement, combined with dynamical measurements in clusters and other estimates of the overall mass density, provides a gauge of the amount of nonbaryonic dark matter in the universe. Furthermore, the degree to which deuterium is depleted in the interstellar medium of our Galaxy and other galaxies provides a tracer of stellar activity. The small isotope shift in the optical lines makes the deuterium measurement extremely difficult and subject to systematic error at optical wavelengths. In contrast, at radio wavelengths the hyperfine lines of deuterium at 327.4 MHz

(92 cm) and hydrogen at 1420.4 MHz (21 cm) are separated by more than a factor of four in wavelength. Detection of the deuterium line (DI) at radio wavelengths will introduce a new tool for studying deuterium abundances.

[3] Several groups have tried to detect the deuterium hyperfine line [Weinreb, 1962]. Weinreb set an upper limit for $N_D/N_H = 8 \times 10^{-5}$. More recent limits by Anantharamaiah and Radhakrishnan [1979], Chengalur *et al.* [1997], Heiles *et al.* [1993], and Blitz and Heiles [1987] are comparable or slightly better. UV/Optical measurements give $N_D/N_H \approx 1.5 \times 10^{-5}$ toward several lines of sight in the interstellar medium [Wood *et al.*, 2004]. For a reliable detection of the 327 MHz line for this D/H ratio, the sensitivity needs to be increased by a substantial factor over that achieved using radio measurements. The noise contribution from radio frequency interference (RFI) plays an important role in achieving the required sensitivity.

[4] The radio emission from the deuterium line is expected to come from the same regions of interstellar

gas that emit the 21 cm line of hydrogen. The best region to search for the DI line in emission is from a region near the galactic anticenter. In this region the opacity is expected to be largest because the velocity dispersion due to the galactic rotation is smallest since the differential motion is largely perpendicular to the line of sight. The emission is expected to be diffuse and spread out over several degrees so that there is no advantage to using a large antenna with a small beam since a smaller antenna whose beam width matches the extent of the emission will receive an equally strong signal. However, to detect the emission, which is expected to be more than 50 dB weaker than the hydrogen line requires many years of integration. For this reason it was decided to design and construct an array of antennas grouped into “stations.” Each station forms a subarray with a beam width that matches the expected extent of the emission. If the stations are separated by a distance equal to a few times their aperture the DI line signals from each station will be uncorrelated. Averaging the spectra from 24 stations taken over 1 year will be equivalent to observing with a single station for 24 years.

2. Characteristics of DI Array

[5] The characteristics of the DI array are summarized in Table 1. The electronics has separate receiver channels for each individual antenna element so that several beams can be steered to track different regions of the sky. The beam-forming software in the PC motherboard is currently limited to calculating four beams. This allows the array to observe several regions simultaneously thereby increasing the efficiency of observing. Aperture

Table 1. Summary of DI Array

	Characteristics
Configuration	Quasi-regular array of 24 stations
Spacing, m	~15
Antennas	5 × 5 (24) compact array of crossed Yagis
Spacing between elements	0.8λ
Collecting area, m ²	12
Beam width	14°
Electronic steering	~±40°, 3 dB
Number of simultaneous available beams	4
Frequency coverage, MHz	322.0–328.6 (centered at 327.4 MHz)
Polarization	Dual linear
System temperature	Limited by sky background 50–400 K
Spectrum, kHz	250 (with 1024 channels, 244 Hz resolution)
Total number of receiver ports	48 × 24 = 1152



Figure 1. View of deuterium array site at Massachusetts Institute of Technology Haystack Observatory.

synthesis using the correlations between stations was initially considered to allow the array to do other projects which require higher resolution but this feature was not implemented owing to limited resources. The array is located in a soccer field–size area on the Haystack Observatory grounds (Figure 1). The location was prescribed by the availability of land and the budget. Since radio frequency interference (RFI) is a major issue at these frequencies, a dedicated RFI monitor has been added and has been in operation since the start of the project. An informal memo series describing the process of the project and the RFI data analysis can be found at <ftp://web.haystack.edu/pub/DI/memoindex.html>.

3. Expected Strength of the DI Line and Array Sensitivity

[6] The expected strength of the DI lines is approximately given by

$$s = 0.27 \times (N_D/N_H) \times (T_{spin} - T_{cont}) \times \tau_H / (T_R + T_{cont}), \quad (1)$$

where

0.27	ratio of line strengths and line widths;
N_D/N_H	deuterium-to-hydrogen abundance (1.5×10^{-5});
T_{spin}	spin temperature (130 K);
T_{cont}	continuum temperature (70 K);
τ_H	hydrogen 21 cm opacity (2);
T_R	receiver noise (40 K).

[7] Substituting the values in parentheses we get a value of 4.4×10^{-6} (4.4 ppm) for the peak expected signal as a ratio of antenna temperature to system noise temperature. A more accurate estimate of 2.6 ppm is obtained from a more complete analysis obtained by convolving the station beam with the measured H1 and continuum data from *Hartmann and Burton* [1997] and *Haslam et al.* [1982], respectively.

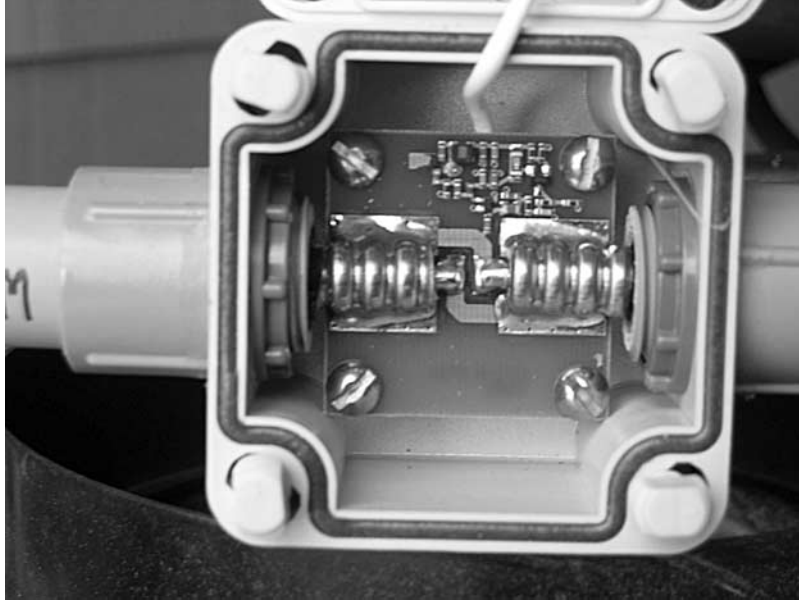


Figure 2. View of the circuit associated with the active dipoles, which includes coaxial stub filters to reduce the susceptibility to the generation of intermodulation products in the low-noise amplifiers.

[8] The more complete analysis effectively includes the effects of beam scan loss and the actual structure of the opacity, continuum and beam shape. The one sigma noise in the spectral average is given by

$$\sigma = (2NbT)^{-1/2}, \quad (2)$$

where

- 2 number of polarizations;
- N number of stations (24);
- b resolution (10 kHz);
- T integration time (10^7 sec).

[9] The one sigma fractional noise is 4.5×10^{-7} assuming the expected 10 kHz width of the DI line and about 2 years observing the galactic anticenter for 4 hours per day. If the DI line is at the expected strength of 2.6 ppm we should then get an SNR of about 5.8 sigma. The expected SNR will be somewhat higher if we use a filter matched to the expected line shape and include the observations of regions one beam width on either side of the anticenter. The integration time is the equivalent “single station single polarization” integration time $2NT$.

4. Controlling Internal Sources of RFI

[10] Careful hardware designs of both the receiver and the active antenna have been done to minimize the RFI

from the internal electronics of both systems. The low-noise active antennas include coaxial stub filters that minimize the RFI coming into the input of the low-noise amplifier (Figure 2). The receiver is in an enclosed box and the analog electronics have been placed in individual boxes within the receiver box. The USB and Ethernet cables have ferrite filters on them, while the AC power has double filtering. The control and data paths are through fiber optic cables to avoid the conduction of RFI out of the receiver box.

[11] In initial testing it was noted that while some of the RFI features that were seen were associated with particular devices, several features were identified as intermodulation (IM) products. Table 2 shows an example of an IM product that was measured in 2002 during the early planning phase of the array. From the signal strengths in Table 2, the input intercept point for the intermodulation product (IIP2) was estimated to be about +8 dBm. As mentioned above, stub filters are used on the

Table 2. Measured Strength of an Intermodulation (IM) Product Close to the DI Line

Frequency, MHz	Source	Level at Input to LNA, dBm
175.26	Channel 7 TV	-65
152.6	Pager	-70
327.86	IM 2	-143



Figure 3. Close-up view of the deuterium array dipoles showing the directors that have been added to reduce the horizon response. Twelve Yagis of the RFI monitor and one set of active antennas pointed at zenith are mounted on the trailer in the background.

active antennas in order to reject low-frequency interference. The addition of these stub filters attenuates the TV and paging channels by about 10 dB, reducing the intermodulation signal to less than -163 dBm. Fortunately this particular intermodulation product, which results from the mixing of two very strong signals, is just outside the 250 kHz wide observing band centered at 327.4 MHz used by the array. However, other weaker intermodulation products are in the observing band and could be detrimental, so every effort has been made to reduce the susceptibility to IM products.

[12] Each receiver channel employs downconversion with a 327 MHz output filter on the preamp to provide over 50 dB out-of-band rejection, a 327 MHz input filter in the receiver for another 50 dB out-of-band rejection and a 50 MHz I.F. filter which provides 50 dB out-of-band rejection. Following the analog-to-digital conversion, a digital down converter filter gives over 100 dB out-of-band rejection in the conversion to baseband. The receiver noise, typically about 40 K, is estimated using a sky brightness model [Rogers *et al.*, 2004].

[13] To reduce the susceptibility to RFI an effort was made to minimize the horizon response of the array. The dipoles were placed over a horizontal ground plane and parasitic directors (Figure 3) were added to reduce the

gain at the horizon by about 10 dB. Placing clutter fences [Rao *et al.*, 2003] around each station was considered, but they needed to be large and would be very expensive.

5. RFI Monitor

[14] In order to characterize the external RFI environment and to develop techniques to identify and mitigate the interference from the data, a monitor has been installed and operated since the beginning of the project. The monitor consists of 12 directional Yagi antennas pointed every 30° around the horizon. This provides not only a detection capability but also the ability to identify the direction of the RFI. In addition, there are two active dipole antennas (replicas of the deuterium array antennas) pointed in the zenith direction (see Figure 3). Further localization of the RFI source is done with a handheld receiver and a variety of antennas, including an active Yagi. Figure 4 shows some sample spectra from the Yagis of the RFI monitor at different azimuths showing that the relative strength of the RFI features provides a measure of the direction of arrival.

6. Characterization of External Sources of RFI

[15] Most of the external sources of RFI have been identified as coming from nearby equipment (such as personal computers) and instrumentation located within 500 m of the array. Digital answering machines and other home electronics within 5 km also introduce strong sources of RFI. Occasional continuum transients mostly of unknown origin have also been detected and these possess spectral features such as those expected from multipath propagation. Figure 5 shows a sample of the complex spectrum produced by a digital modem at a nearby site. This modem has been replaced by another which generates little or no RFI in the 327 MHz band. It is obvious that unless some of these sources are controlled or eliminated, any excision technique would result in the loss of a large amount of data.

[16] Many of the RFI signals were identified as coming from nearby homes and offices. Several measures have been taken to control the RFI at the source including negotiating with neighbors to replace certain consumer products which have clock harmonics close to 327 MHz. In addition, buildings on observatory grounds within 500m of the array have been shielded.

[17] Most of the RFI from consumer products are narrowband, “continuous wave” (CW) signals, which have a simpler spectrum than that of the modem shown in Figure 5. In Figure 6 we show RFI at 327.400 in the top plot for an azimuth of 150° . The signal was first detected in the RFI monitor antenna pointed at an

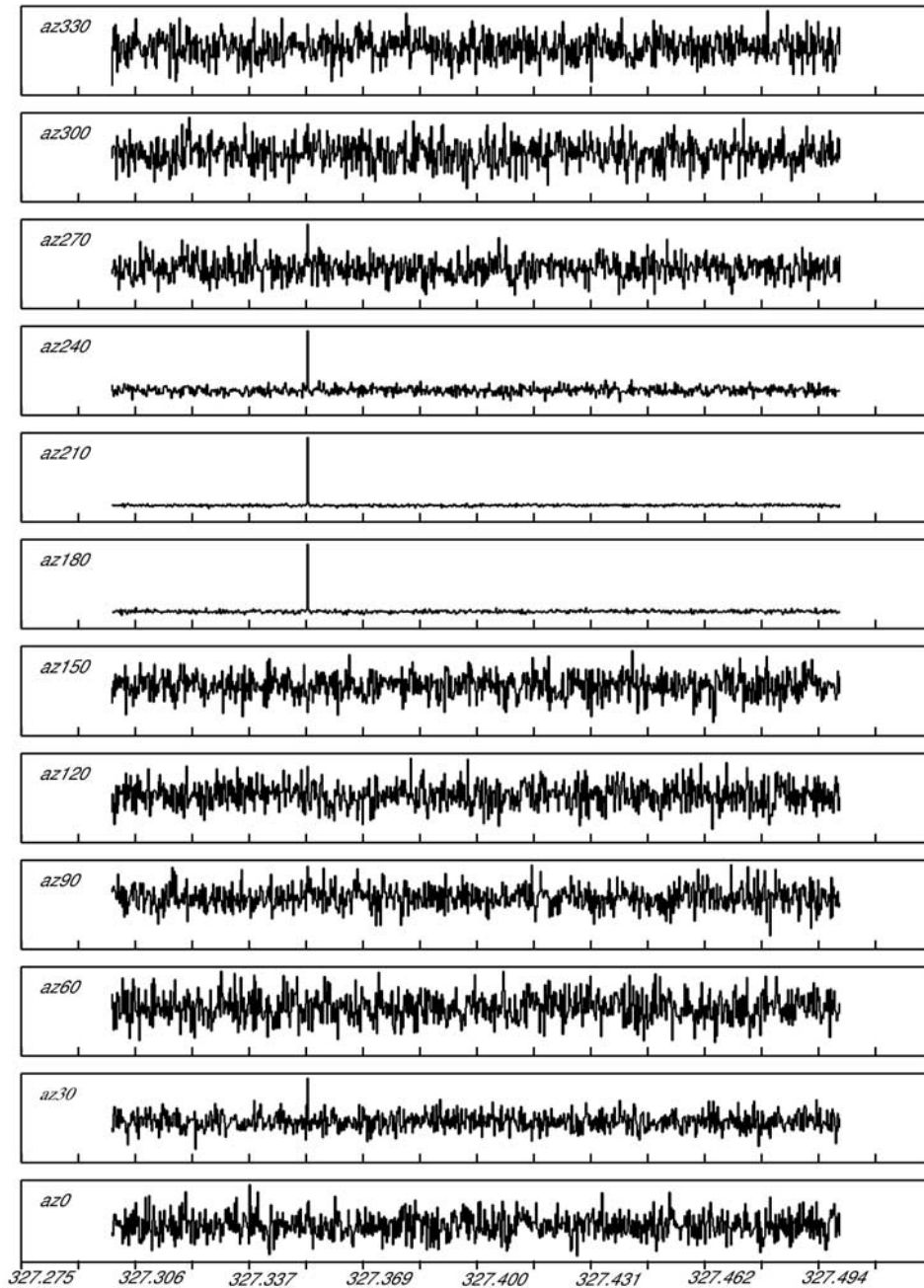


Figure 4. Sample plot from the RFI monitor showing a strong interference spike in some channels. This information is used in determining the direction of the interference.

azimuth of 150° . The source of the RFI was then identified by following a path along the azimuth indicated by the monitor with a handheld receiver connected to an active Yagi antenna. The signal is produced by the 29th harmonic of the 11.2896 MHz clock in a CD player part of a surround sound system located in a house about

2 km from the array. The signal strength at the RFI monitor is about -170 dBm. The estimated effective isotropic radiated power (EIRP) at the source is about -97 dBm assuming a Yagi gain of 13 dBi and a free space path. The bottom plot in Figure 6 shows a somewhat stronger signal at 327.351 MHz coming from

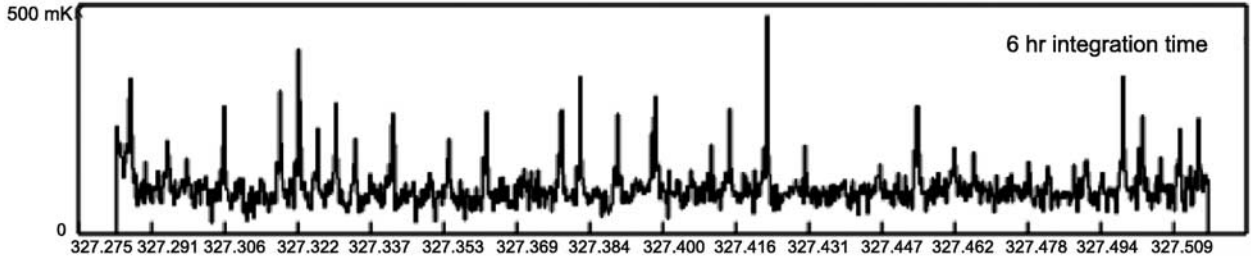


Figure 5. Plot from one channel of the RFI monitor showing the interference from a digital modem at the Westford radio telescope site, which is about 180 m away. Any RFI source whose effective isotropic radiated power is greater than about -97 dBm at 100 m will be stronger than the deuterium line.

an azimuth of 210° . In this case the signal was from an answering machine in another house also about 2 km away.

7. Effect of RFI on Data From the Array

[18] Signals which are as strong as those seen in Figure 6 are expected to be present in the individual dipoles of the array at about a level of 23 dB below that seen by the RFI monitor because the dipole response at the horizon is about -10 dBi. As a result these signals can only be seen when many days of data from all the dipoles are averaged. The beam has a gain of about 22 dBi, so the effect of the signals such as those in Figure 6 are expected to be much less. A -190 dBm signal seen in the monitor is expected to be about -203 dBm or 18 ppm in the beam. While such signals can only be seen in very

long integrations they are significant in the search for the DI line and these CW-like features need to be excluded from the spectral averages as described in the next section.

8. Mitigating RFI in the Deuterium Array Data

[19] While the major sources of RFI are identified and controlled at the source, residual RFI features are excised through data processing techniques. In the case of transient sources, any spectral or continuum signal that exceeds the 8 sigma level in the RFI monitor is excised in the data from the deuterium array channels. Continuum transients can produce spectral features due to multipath. An example of a continuum transient is shown in Figure 7. These transients can be excised using the

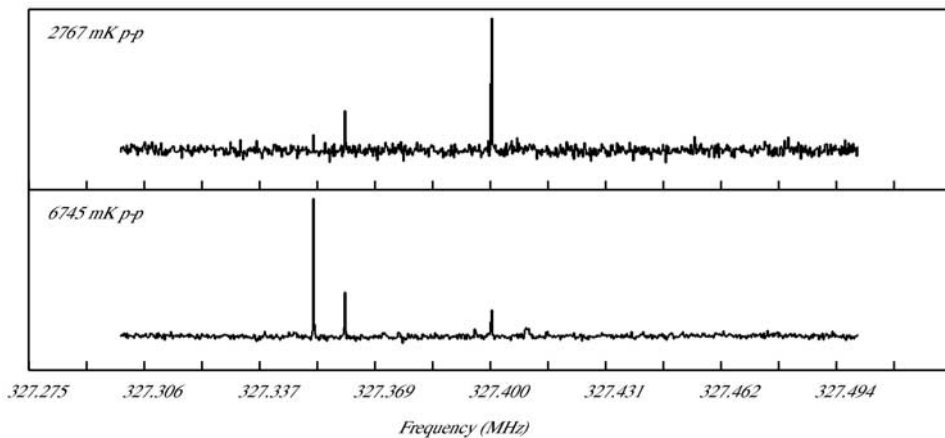


Figure 6. Examples of two sources of narrowband RFI. These spectra are 24 hours integration taken on 9 March 2004.

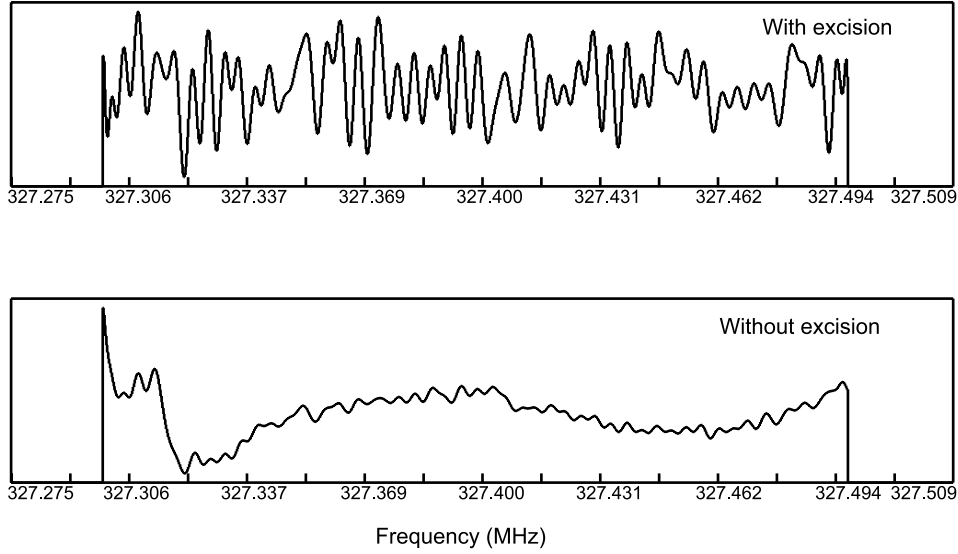


Figure 7. Example of excision of a continuum RFI transient with multipath. The peak-to-peak variation in the spectrum is reduced from 2630 to 509 ppm.

variation in the curvature from a polynomial fit to the spectrum as a measure. In the example of Figure 7 the excision of all data with more than 8 sigma of curvature removes the spectral ripple produced by the transient. For narrowband features that are seen in frequency space, spectral exclusion is performed on any of the 244 Hz resolution frequency channels in the array data for which RFI is detected above the 8 sigma level in 24 hours of integration. A weighted least squares smoothing to 2 kHz resolution is used to “interpolate” over the excluded frequency channels for each day’s integration.

[20] The details of this method are as follows: The vector describing the original spectrum, X can be written as

$$X = As + n, \quad (3)$$

where A is the steering or design matrix, s is the vector of model coefficients, and n is the error vector. A weighted least squares solution to equation (3) which minimizes chi-square is given by

$$\hat{s} = (A^H w A)^{-1} A^H w X \quad (4)$$

$$\hat{X} = A \hat{s}, \quad (5)$$

where w is the weight matrix with all off diagonal elements equal to zero for which $w_{ii} = 1$ for accepted points and $w_{ii} = 0$ deleted points. H denotes the hermitian conjugate and -1 the inverse of the matrix. \hat{X} is the smoothed spectral estimate.

[21] Since the spectrum is real it is convenient to make the smoothing function

$$A_{ij} = \cos(\pi x j) \text{ for even values of } j \geq 0 \text{ and } j < 128 \quad (6)$$

$$= x \text{ for } j = 1 \quad (7)$$

$$= \sin(\pi x (j - 1)) \text{ for odd values of } j > 1 \text{ and } j < 128, \quad (8)$$

where $x = (i - fstart)/(fstop - fstart)$. $fstart$ and $fstop$ are the desired start and stop indices in the original 1024 point unsmoothed spectrum.

[22] The expected error in the Fourier coefficients is given by the covariance

$$\begin{aligned} (\hat{s} - s)(\hat{s} - s)^H &= (A^H w A)^{-1} A^H w n n^H w^H A (A^H w A)^{-1} \\ &= (A^H w A)^{-1} \sigma_0^2 \end{aligned} \quad (9)$$

since

$$(n n^H)_{ij} = \sigma_0^2 \text{ for } i = j \quad (10)$$

$$= 0 \text{ for } i \neq j \quad (11)$$

$$w w^H = w \text{ since } w_{ii} = 1 \text{ or } 0. \quad (12)$$

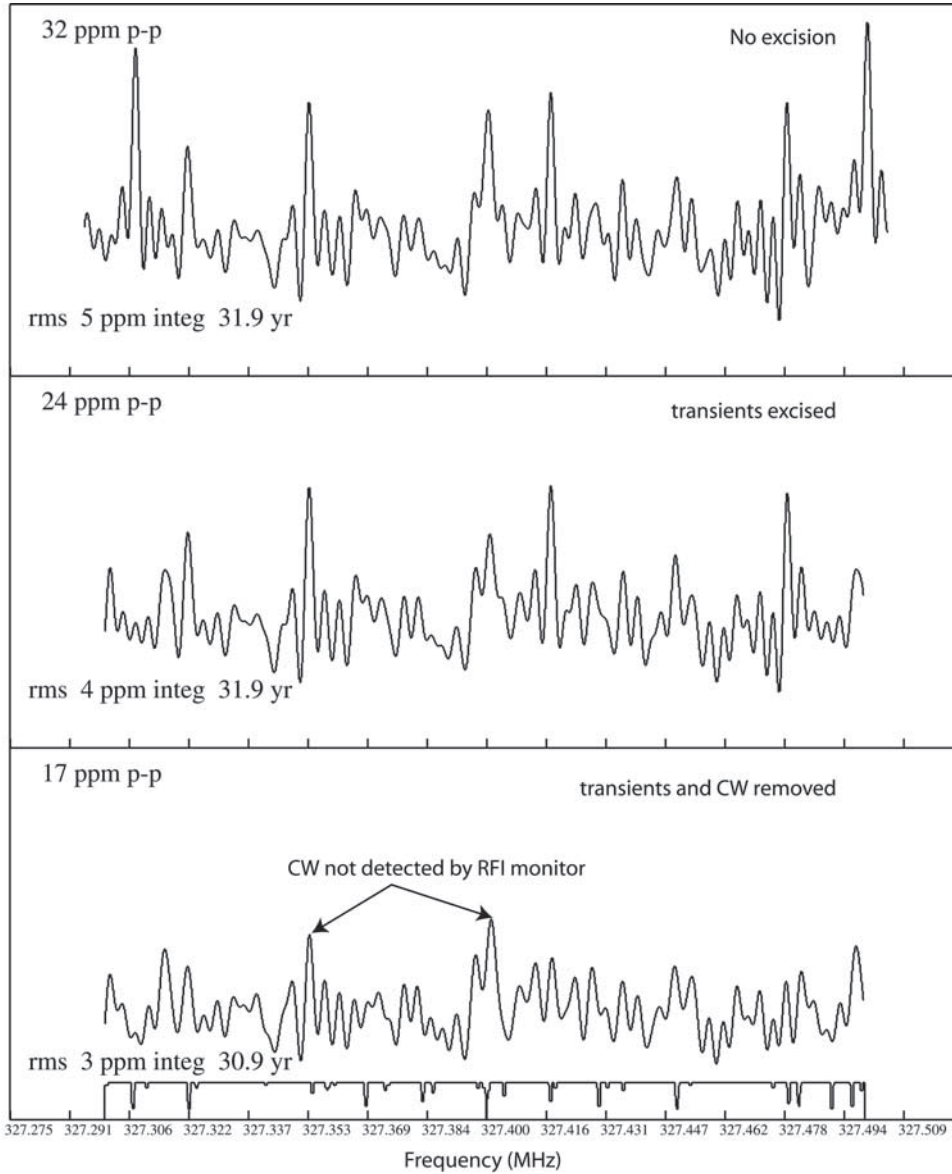


Figure 8. Example of the RFI excision technique. The resolution has been smoothed from 244 to 2 kHz. The amplitude scales are in units of parts per million (ppm) of the system noise.

The spectrum of the estimated error is given by the diagonal elements of the transformed covariance matrix

$$\sigma_i = \left[\left(A(\hat{s} - s)(\hat{s} - s)^H A^H \right)_{ii} \right]^{1/2} \quad (13)$$

$$\sigma_0 = \left[\left(A(A^H w A)^{-1} A^H \right)_{ii} \right]^{1/2} \sigma_0,$$

where b is the original spectrum resolution = 244 Hz, T is integration time, and

$$\sigma_0 = (bT)^{-1/2}. \quad (14)$$

[23] The effect of excluding a few narrowband 244 Hz channels is minimal unless many adjacent channels are excluded. For example, if six adjacent channels are excluded, the noise will increase by up to a factor of

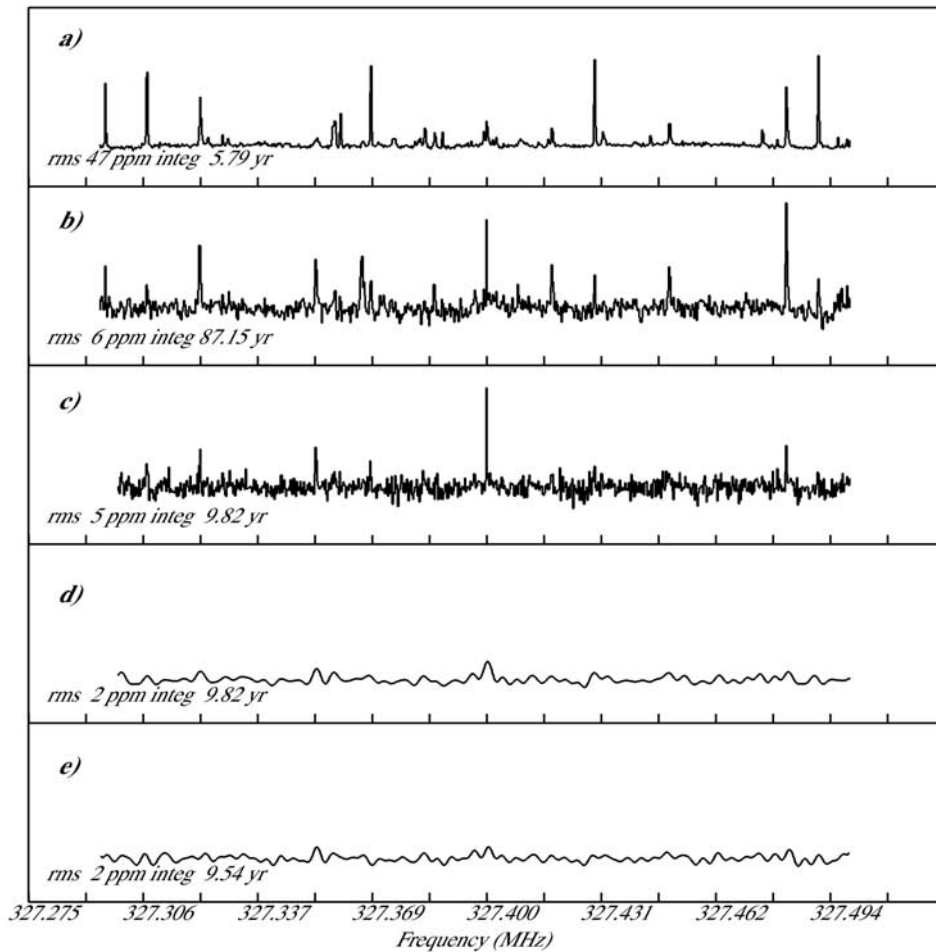


Figure 9. Mitigation of RFI from data taken from 9 April 2004 through 9 October 2004: (a) average spectrum from all RFI monitor ports after excision of transients over 8 sigma in 100 s, (b) average spectrum from all array dipoles after excision of transients over 8 sigma in 500 s, (c) average spectrum of all reference beam data after transient excision, (d) spectrum in Figure 9c after smoothing to 2 kHz resolution, and (e) average spectrum from all reference beam data with the exclusion of spectral channels with RFI detected by the RFI monitor. Figure 9a has a full-scale value of 1000 ppm (~ 200 mK), while the remaining plots have a full-scale value of 80 ppm (~ 8 mK). Integration times are all “equivalent” times.

two in the region of the spectrum around the excluded channels. The exclusion of a single channel results in less than a 10% local increase in the noise. In another example, if every other 244 Hz channel were excluded, the noise would increase by the square root of 2 everywhere in the spectrum. A sample result of this excision technique is shown in Figure 8 for the case of the average spectra from all the individual elements of the array. Averaging data from all 1152 elements gives an equivalent “simple element” integration of over 30 years and is a good test of the RFI mitigation. It should be emphasized that averaging the spectra from all of the

elements of the array, as shown in Figure 8, only provides a means of measuring the influence of RFI.

9. Effect of RFI on Station Beams

[24] The dominant RFI is transient in nature and it is essential to excise the time spans with strong RFI. Figure 9 shows the example of all the beam data taken from reference positions from 9 April 2004 through 9 October 2004 with and without complete RFI excision. The “reference” beam data is data taken away from the Galactic plane and is not expected to have significant DI

emission. With RFI excision the RMS noise in the spectrum, which as been smoothed to a resolution of 2 kHz for the spectral exclusion, is 2 ppm which is close to the theoretical value.

[25] In the operation of the array, the spectra from the beams formed by each station are averaged. At any instant the software running at each station processes simultaneous beams in four different directions, each with two polarizations. This allows the simultaneous observation of regions like the Galactic anticenter, where we expect to detect the deuterium line, along with other regions which can be used for reference or comparison. While the level of RFI still evident in Figure 8 is quite significant, the beams that track the sky have more than 10 dB additional rejection of RFI over that seen by the individual dipoles. Therefore if we can reduce the effect of RFI to a few parts per million (ppm) in the spectra from the individual dipoles we can be confident that its effect on the spectra from the station beams will be well below the 3 ppm signal expected from the deuterium line. With a few months of operation, we have the equivalent of several years of integration time in the data from the 48 beams. However, because of the added rejection of signals from the horizon by the beams, the bottom spectrum shown in Figure 9 which has RFI excision in time and frequency shows little if any evidence of RFI contamination. The caveat to this conclusion is that during the spring and summer months of the observations taken so far the array has been surrounded by heavy foliage so that the general RFI environment is about 6–10 dB quieter than is expected in the winter months when the trees are bare. In that situation, it is expected that more RFI signals, both transient and continuous wave (CW) will be detected and will have to be suppressed. The transient excision results in a loss of about 10% of the data while the spectral exclusion increases the noise by a few percent.

[26] In the search for the DI line the spectra have the frequency axis transformed to velocity relative to the local standard of rest before being averaged. Statistically significant results from this search are not yet available since we have not yet acquired sufficient data.

10. Conclusions

[27] MIT Haystack Observatory has recently completed the construction of a dedicated array to detect the 327 MHz line of deuterium. Detecting, characterizing and excising RFI has been the challenge of the early part

of this project. Currently, the combination of removing strong and persistent sources of RFI at the source and excising transients in the data has resulted in the successful elimination of most of the RFI in the deuterium array data.

[28] **Acknowledgments.** The deuterium array project at MIT Haystack Observatory has been supported by the National Science Foundation (grant AST-0115856) and MIT.

References

- Anantharamaiah, K. P., and V. Radhakrishnan (1979), A new upper limit to the abundance ratio of atomic deuterium to hydrogen in the direction of the galactic centre, *Astron. Astrophys.*, *79*, L9–L11.
- Blitz, L., and C. Heiles (1987), A new assault on the 92 centimeter line of DI, *Astrophys. J.*, *313*, L95–L98.
- Chengalur, J. N., R. Braun, and W. B. Burton (1997), DI in the outer galaxy, *Astron. Astrophys.*, *318*, L35–L38.
- Hartmann, D., and W. B. Burton (1997), *Atlas of Galactic Neutral Hydrogen*, Cambridge Univ. Press, New York.
- Haslam, C. G. T., C. J. Salter, H. Stoffel, and W. E. Wilson (1982), A 408 MHz all-sky continuum survey II: The atlas of contour maps, *Astron. Astrophys. Suppl. Ser.*, *47*, 1–143.
- Heiles, C., P. R. McCullough, and A. E. Glassgold (1993), Radio observations of DI and fractionation, *Astrophys. J.*, *89*, 271–292.
- Rao, Q., H. Hashiguchi, and S. Fukao (2003), Study on ground clutter prevention fences for boundary layer radars, *Radio Sci.*, *38*(2), 1030, doi:10.1029/2001RS002489.
- Rogers, A. E. E., P. Pratap, E. Kratzenberg, and M. A. Diaz (2004), Calibration of active antenna arrays using a sky brightness model, *Radio Sci.*, *39*, RS2023, doi:10.1029/2003RS003016.
- Weinreb, S. (1962), A new upper limit to the galactic deuterium to hydrogen ratio, *Nature*, *195*, 367–368.
- Wood, B. E., J. L. Linsky, G. Hebrard, G. M. Williger, H. W. Moos, and W. P. Blair (2004), Two new low galactic D/H measurements from the far ultraviolet spectroscopic explorer, *Astrophys. J.*, *609*, 838–853.

J. C. Carter, P. Pratap, and A. E. E. Rogers, Haystack Observatory, Massachusetts Institute of Technology, Westford, MA 01886, USA. (aeer@newton.haystack.edu)

M. A. Diaz, Department of Electrical and Computer Engineering, One Sherborn Street, Boston University, Boston, MA 02215, USA.